A contamination-free electrolyte-gated organic transistors platform for high-accuracy tumor biomarker detection

Sensors and Actuators Reports 9 (2025) 100341

Contents lists available at ScienceDirect

Sensors and Actuators Reports

journal homepage: www.sciencedirect.com/journal/sensors-and-actuators-reports

A contamination-free electrolyte-gated organic transistors platform for high-accuracy tumor biomarker detection

Jovana Babic [a], Alberto Ballesio [a,b,*], Francesca Frascella [a,c], Lucia Napione [a,c], Mattia Pagani [a], Matteo Parmeggiani [a,1], Simone Luigi Marasso [a,b]

[a] DISAT – Politecnico di Torino, Corso Duca degli Abruzzi 24, 10129 Turin, Italy
[b] CNR-IMEM, Parco Area delle Scienze 37, 43124 Parma, Italy
[c] PolitoBIOMed Lab, Politecnico di Torino, C.so Duca degli Abruzzi 24, 10129 Turin, Italy

ARTICLE INFO

Keywords:
Angiopoietin 2
OECT biosensor
Cancer biomarker
Microfluidics
Electrochemical biosensing

ABSTRACT

A novel biosensor platform for high-accuracy tumor biomarker detection exploiting contamination free microfluidics for increasing the signal-to-noise ratio has been successfully developed and tested. Electrolyte-gated organic Transistors (EGOT) has been employed to detect an important tumor marker, Angiopoietin-2 (Ang2). Although organic semiconductors have become popular in the last years in biosensing applications due to their many advantages, there is still a main concern about stability and selectivity. This work presents major improvement in terms of the stability and selective detection of Ang2 in the range of interest for biomedical applications. The semiconducting polymer poly[3-(5-carboxypentyl)thiophene (P3CPT) is deposited by picoliter volume control and micrometer diameter of the droplet to allow for high uniformity and repeatability from sample to sample. The optimized gold electrodes improve the detection of the minimal concentration of the target and microfluidic interfacing by a specific pattern with the desired dimensions is obtained by UV-lithography and wet etching. A microfluidics with multiple flow control allows for maintain a constant fresh solution without analytes on reference gate electrode, while another inlet and functionalized gate is used for sensing, thus reaching high stability and reproducibility. All these (four) optimizations lead to new measuring protocol and new 3D printed top cover that ensure better stabilization and repeatability of the results. The device has successfully detected Ang2 concentrations as low as 10 pM in saline, therefore demonstrating the ability of the device to detect clinically relevant concentrations.

1. Introduction

Cancer is a leading cause of death worldwide, accounting for nearly 10 million deaths in 2020 [1].The detection of protein biomarkers has promising potential for early diagnosis and monitoring of diseases such as cancer. Today, most clinical protein biomarker detection is done using enzyme-linked immunosorbent assays (ELISAs) [2], but requirements for relatively expensive test kits and bulky plate readers limit ELISA's usefulness for point of care (POC) diagnostics [3].

In recent decades, BioElectrochemical Detection, has been progressively gaining attention as methodology for the detection of biomarkers and electrolyte biosensors have been rapidly developed. Electrolyte gated transistor biosensors combined with microfluidic channel can be a perfect candidate as they have many advantages such as portability, low power consumption, simple instrumentation and fast response. In addition, they show excellent sensitivity and selectivity, low detection limit, and good stability over time. Very often small molecules can be detected by this technique at high sensitivity, because their presence generates an electron transfer proportional to their concentration. This type of biosensor has been used for detection of lactate, glucose, and cholesterol [4], in vitro cell monitoring [5], metabolite sensing [6]. Additionally, electrolyte gated transistors exploit mostly organic semiconductors as they possess excellent biocompatibility, flexibility, easy processing, and molecular diversity [7]. This type is called Electrolyte gated organic transistors – EGOTs. Usually, a label is used to identify protein biomarkers and to achieve high selective recognition of the target. Indeed, a label-free analysis can be done only for electro-active compounds as in this case. For all the other analytes, the sensing is

* Corresponding author.
E-mail address: alberto.ballesio@polito.it (A. Ballesio).
[1] Current affiliation is different respect to the one in which the work was done.

https://doi.org/10.1016/j.snr.2025.100341
Received 21 February 2025; Received in revised form 29 April 2025; Accepted 25 May 2025
Available online 25 May 2025

mediated by other molecules. Label free detection makes the whole sensing procedure a lot faster and simpler.

EGOTs based biosensors are three-terminal devices, where the current measured between source and drain (I_{DS}) is modulated by the functionalized gate electrode. The main mechanism is based on the coupling between the Electrical Double Layer (EDL) that occurs at the interface between the electrolyte and the active material (i.e. organic semiconductor) and the EDL that occurs at the interface between the electrolyte and the gate electrode. When ions cannot diffuse inside the transistor channels the application of a voltage to the gate electrode causes migration and accumulation of ions at the gate-electrolyte and at the semiconductor-electrolyte interfaces, in this case, the device is called Electrolyte Gated Organic Field Effect Transistor (EGOFET) and the result is that charges stored in the latter EDL will modulate the drain current of the device. On the other hand, when ions can penetrate inside the transistor channel, application of a voltage to the gate electrode may cause the injection of ions in the organic semiconductor, resulting in an electrochemical doping/dedoping of the material. In this case the current of the device is electrochemically modulated and the resulting devices are called Organic Electrochemical Transistors (OECT). However, often the working mechanism of EGOTs is characterized by a mixture of field effect operation and electrochemical operation, as in the case of devices exploiting P3CPT as organic semiconductor [8],[9]. The use of these devices as biosensors implies the study of the main figures of merits as well as the sensitivity and the selectivity towards specific biomarkers. A lot of works successfully find good results on significant biomarkers [10–13], however it is difficult to go down below a certain threshold without workarounds as sample pre-concentrations [14]. In general, by capturing the biomarkers on the functionalized gate electrode surface, the capacitance of the EDL at gate electrode/electrolyte interface will be altered, leading to a change in the potential, ΔV_{GS}, thus changing the output current. This way, a shift of the output current can be associated with the concentration of the analyte biomarker in the sample being tested. In the last years, organic transistors have been successfully used as monitoring of harmful factors in the environment [15], proteins [16], drugs [17]. In this work, the solutions adopted allow to go below limits of detections shown in previous works without pre-concentration or particular escamotages [18], but only by referring the sensing measurements to a stable reference and using a well-tested microfluidics [19] .

Among tumor biomarkers, Ang2 was selected as it is of special interest to researchers and clinicians. More specifically, Ang2 is a factor belonging to the angiopoietin/Tie signaling pathway, one of the main pathways involved in angiogenesis [20]. In particular, it has been reported that i) Ang-2, in collaboration with vascular endothelial growth factor (VEGF), initiates angiogenesis by destabilizing existing blood vessels, ii) Ang2 expression is restricted in healthy subjects, while its level is elevated in cancer patients, which correlates with poor prognosis [21] and iii) early modulation of Ang2 levels may predict benefit from drug treatment in cancer patients [22].

This work was initiated based on a previously developed microfluidic platform [23]. In [23] the optimization of the flow was performed in order to obtain stable and reproducible results. Originally, the device was composed of 2 p.m. covers, microfluidic channels, a biosensor chip, and two non-patterned gates. Measurements were performed using micromanipulators connecting to Signal-measuring unit (SMU) by measuring the output current. Three distinct chambers were embedded in the construction of a microfluidic chip: one housing the sensor made of OSC material, another housing the sensing gate electrode and a third one used for the reference. The top cover and PDMS microfluidics contained two inlets: one for the analyte-containing solution and another one for the blank buffer. The microfluidic geometry design prevented the transistor channel contamination as the analyte can only flow in the direction of the sensing gate chamber. Although this design was already good to avoid contamination on organic semiconductor channel, it failed in terms of reproducibility. For this reason, we further improved this concept for higher performance both in terms of sensitivity and reproducibility of the result. In particular, in the present work four new improvements are carried out at the same time in order to increase the stability and the reproducibility: i) optimizations regarding organic semiconductor deposition, ii) gate patterning, iii) integrated contacts, and iv) new measurement protocol with stabilization time, developed following the study of electrical bias stress in EGOTs [9]. All these innovations have led to a device configuration that is able to detect and quantify different concentrations of Ang2 biomarker in the diluted in PBS.

2. Materials and methods

2.1. Fabrication

2.1.1. Microfluidics and holders

The microfluidic platform concept was already developed elsewhere [23]. In brief, microfluidics is made of PDMS through replica molding by means of two masters: one for the bottom part that defines the microfluidic channels and the opening windows; the other master is for the top part which is used as sealing cap. The opening windows define the exposed area of both the sensor and the gates, and they were set to 9 mm^2 for both. The masters are fabricated by the 3D printer (Objet30 by Stratasys®, Stratasys Ltd., Eden Prairie, MN, USA) using Vero White photosensitive resin (Stratasys, Ltd., Eden Prairie, MN, USA) and post cured as reported in previous works [24]. The PDMS (Sylgard 184, with a 10:1 mass ratio between the elastomer and the curing agent) is then cast into the two masters and placed in the oven for 1 hour at 90 °C to allow for polymerization. After baking in the oven, they are carefully extracted from the two masters and bonded together by the thin layer of no polymerized PDMS and returned to the oven for about 30 min to reduce leakages.

The particular microfluidics design allows for delivering only the solution with analyte to be tested on one inlet and only fresh buffer solution on the reference electrode (Fig. 1a). In this way, the injected analyte from Inlet 2 will flow only over functionalized gated and flow out through the outlet, thus non contaminating the sensing element of the biosensor (i.e. the channel).

To place each part of the device at the correct position, as well as to ensure that the fluidics is well protected and sealed, the top and the bottom holder are fabricated. The bottom holder is a PMMA holder cut by the CO_2 laser. On the other hand, the top one was optimized and designed in order to allow contacts to be integrated and fixed (Fig. 1b). Indeed, it is fabricated using the 3D printer (Objet30 by Stratasys®, Stratasys Ltd., Eden Prairie, MN, USA). This new configuration allows for quicker measurement and more importantly reproducibility of the results with higher precision as the measurements are always taken at the same points on the electrode gates and sensor contacts (Fig. 1c).

2.1.2. EGOT

Chip fabrication also follows typical cleanroom process, as previously reported [23]. Shortly, biosensor is fabricated in the cleanroom starting from the p-doped 4-inch Si-SiO_2 wafer with a 1 μm SiO2 coating thermally grown on top of Si. After spincoating of 10 nm Ti adhesion layer, AZ 5214 E image reversal photoresist was spin-coated and exposed to UV light to transfer the desired pattern. After removal of unwater parts of photoresist, 100 nm thick layer of Au was evaporated, followed by a lift off process. This way, a channel of 9960 μm length and 10 μm width is obtained. Following the same protocol, second lift-off process is performed in order to deposit a passivation layer of Al_2O_3. Detailed process is described in Supplementary material.

The organic semiconductor used with this biosensor was poly [3-(5-carboxypentyl) thiophene-2,5-diyl] (P3CPT). Respect to previous deposition protocol [9], a semiconductor ink was formulated for the deposition by an ink-jet printer (MicroFab Technologies Inc, Texas, US). The solid P3CPT was dissolved in dimethyl sulfoxide (DMSO) to achieve

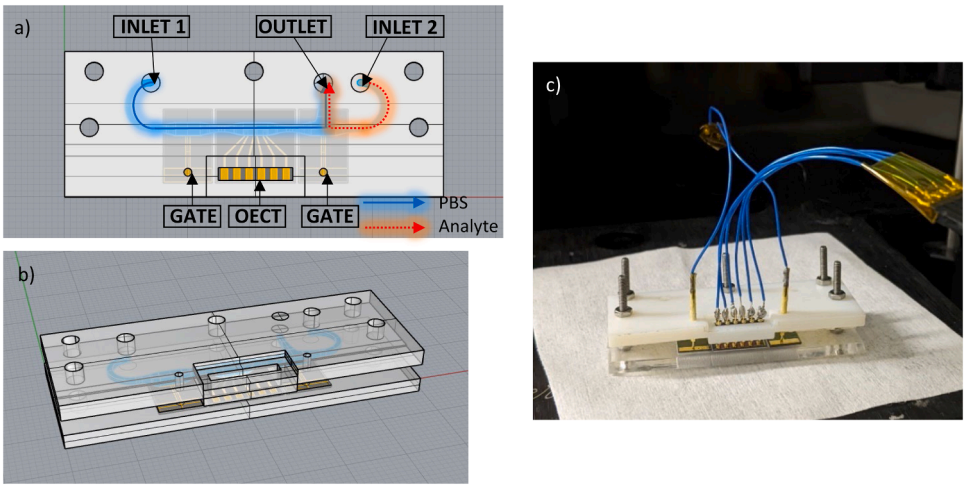

Fig. 1. a) Top view of the microfluidic platform. The PMMA bottom holder accommodating EGOT sensor and two electrodes (reference and sensing). Microfluidics, with two inlets and an outlet, is placed on top of them. The top cover is 3D printed and contains holes for the contacts' bonding. b) 3D view. c) Real view.

a concentration of 0.5mg/mL, then ink-jet printed directly on the chip. The optimized parameters for the jetting device driving were reported in Table S1 and the voltage signal is graphically represented in Figure S2, in supplementary material.

Once P3CPT is deposited (Fig. 2) applying the parameters in tables S1 and S2, the chip was carefully maintained in dark environment and then cured at oven for 2 h at 75 °C. This slow drying allows for the formation of a uniform thin film, avoiding the so called "coffee stain effect", thus better detection accuracy and improved sensitivity.

2.1.3. *Gates patterning and functionalization*

The device exploits two gold electrodes (Fig. 1): sensing and reference gates. The fabrication for letters follows the same steps of chip electrode fabrication. Briefly, a lift-off process is employed to obtain "T" pattern (Fig. 3a) a 10 nm thick Ti layer is e-beam evaporated as adhesion layer, followed by a 100 nm thick Au layer deposition. Then the wafer is left for 30 min in acetone to remove the photoresist and finalize the electrodes patterning. The wafer was then diced (Microla Optoelectronics Srl, Chivasso, Italy) in order to obtain a rectangular gate electrode with dimensions 7.8 mm x 11.8 mm (Fig. 3b). In this way, the same area of the gate is always employed and there will be a better comparison between reference and sensing gate. By refining the electrode design, the platform now provides a more stable and consistent signal output with respect to the old platform.

To enable specific biomolecule detection, both gate electrodes underwent a functionalization protocol based on self-assembled monolayers and antibody immobilization (Fig. 4). In short, main steps include:

1. SAM Formation: Gold electrodes were cleaned (acetone, 2-propanol, N_2 dried) and incubated in 10 mM 3-MPA thiol solution for 1 hour to form a Self-Assembled Monolayer (SAM).
2. Surface Activation: Carboxyl groups on the SAM were activated using EDC/Sulfo-NHS chemistry in MES buffer (pH 4.7), enhancing reactivity toward primary amines.
3. Antibody Immobilization: Electrodes were incubated overnight at 4 °C with anti-Ang2 antibodies (5 μg/ml in PBS), followed by washing with PBS-Tween and drying.

Full functionalization protocol is described in the Supplementary material, chapter 2.

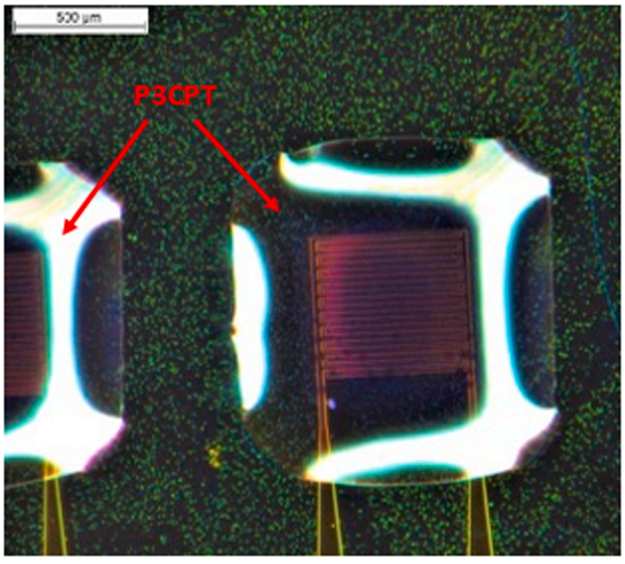

Fig. 2. P3CPT deposited on the interdigitated channel of the transistor chip via Inkjet before it dried.

2.2. *Electrical characterization*

The whole device is placed on the probe station where it's connected by the three crocodile triaxial cables to the Keysight B2912A Precision Source/Measure Unit (SMU), Keysight Technologies. Keysight B2912A supports two channels. In our case, both are applying voltage and measuring the current. The first channel, CH1, applies V_{DS} and measures drain-source current IDS. The other one is used to apply V_{GS} and measure gate current I_{GS}. Source is grounded, the drain and gate voltage are set by the source unit. SMU is controlled by the software Keysight B2900 Quick IV Measurement Software, by Keysight Technologies.

During biosensing measurements, the drain-source voltage V_{DS} is held at constant voltage and gate-source voltage V_{GS} applied as a sweep. V_{DS} is applied through Channel 1 from QUICK IV software and set at value −0.6 V. At Channel 2 it is applied a voltage sweep for V_{GS} from 0 V to −0.6 V as a pulsed signal with a pulse width of 0.202 s. The pulsed measurement procedure has been proven to minimize the bias stress effect on the device [9]. These measurements are repeated five times in order to obtain stable current value. Both drain-source I_{DS} and gate I_{GS} currents are measured (Figure S2 and S3). I_{GS} should be as low as possible and at least two orders of magnitude lower than I_{DS}. Higher gate leakage current may arise from liquid leakages short circuiting the device, or from the failure of the Al_2O_3 passivation layer.

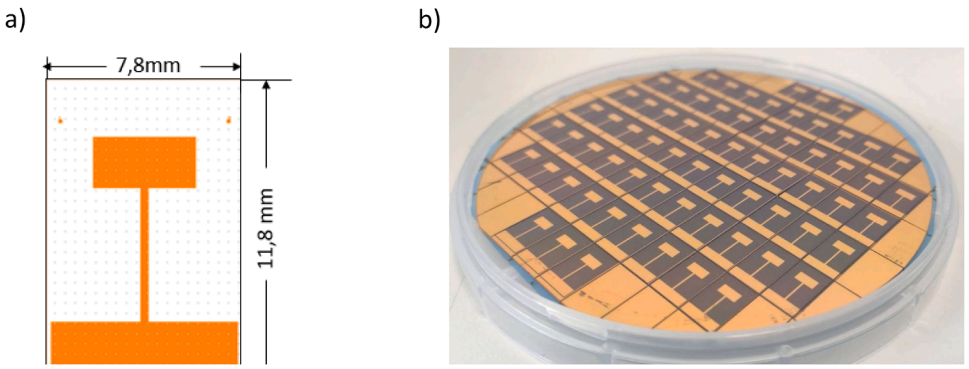

Fig. 3. a) top view of the CAD patterned gate; b) diced wafer with the patterned gates.

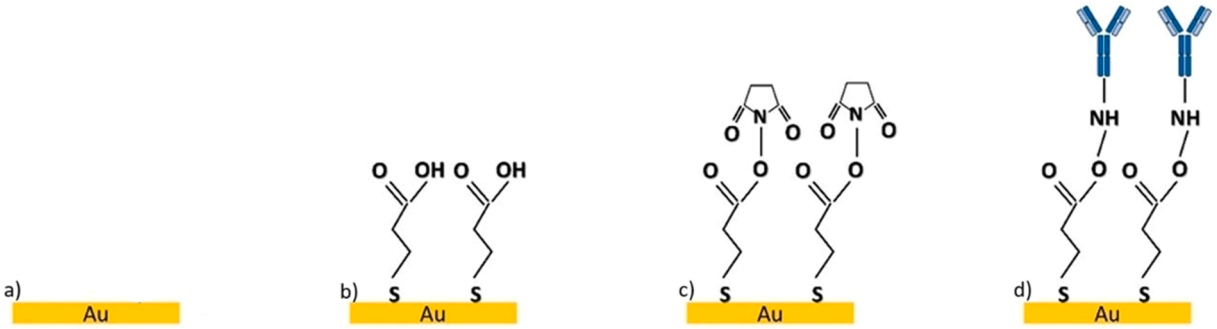

Fig. 4. Functionalization protocol and binding strategy. Au gate functionalization with anti-Ang2 antibody. a) Bare gold electrode. b) formation of the self-assembled monolayer (SAM) of thiols on Au surfaces. c) Activation of the carboxylic group by carbodiimide. d) Final decoration with anti-Ang2 antibody.

2.3. Biosensing protocol

The whole device is placed on the probe station and the microfluidic platform with the chip is then connected to the SMU (Fig. 5). Before biosensing tests, chips were tested in order to verify correct functioning and stability of the devices. The applied voltage signal and obtained output and transfer characteristics are full reported in Supplementary material. Inlet 1 is connected to the syringe pump for delivering PBS 0.01x with a flow rate of 100 μL/min until the microfluidic channel is completely full, after which the measurement from 3.2. is performed for all three devices with both reference and sensing gates. After 10 min, the same measurements are repeated. The signal S, for reference and sensing gate, is calculated as:

$$\mathrm{I(max)(\%)} = \frac{\Delta I}{I} = \frac{Imax_{i} - Imax_{i-1}}{Imax_{i-1}} \quad (1)$$

where i is the number of measurements. If $\frac{\Delta I}{I}(\%) < 5\%$ the sensor is working properly, and it is ready for biosensing measurement. Then, Inlet 2 is connected to a peristaltic pump through which solution with a target, Ang2 (Recombinant Human Angiopoietin-2, R&D System, Milan, Italy, cat. 623-AN/CF), is delivered at different concentrations to the sensing gate chamber with a flow rate of 30 μL/min until the drop starts flowing out through the outlet, after which the flow is stopped to allow incubation of the analyte onto the functionalized gate surface. Finally, after 30 min, again from inlet 1, flux PBS with the speed of 100 μL/min for 10 min to wash away all the molecules not specifically bounded. Devices are measured once again for both gates and $\frac{\Delta I}{I}$ is measured with

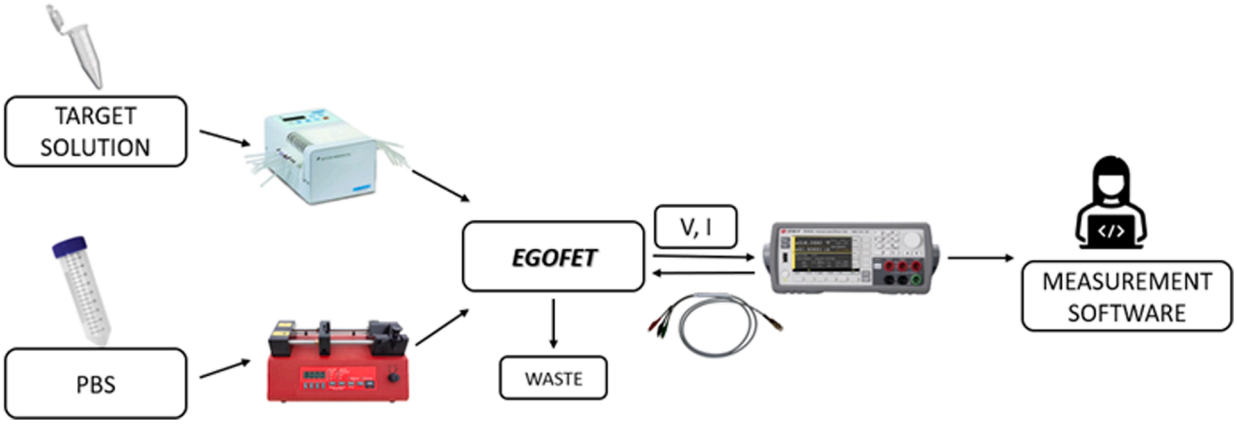

Fig. 5. Schematic representation of the measurement set up.

respect to the last PBS measurement. If the devices are working properly, $\frac{\Delta I}{I}$ of the functionalized gate should change and $\frac{\Delta I}{I}$ of the reference gate should keep the value before analyte incubation.

3. Results and discussion

3.1. Electrical characterization

Transcharacteristics were performed for drain voltage of −0.1, −0.2, −0.3, −0.4, −0.5 and −0.6 V and a gate voltage ranging between −0.2 V and 0.6 V (Fig. 6a). Output characteristics were acquired for gate voltages of −0.1, −0.2, −0.3, −0.4, −0.5 and −0.6 V and a drain voltage between was swept between −0.6 V and 0.0 V (Fig. 6b). All measurements were carried out using PBS 0.01x as electrolyte.

During biosensing measurements, the drain-source voltage V_{DS} is held at constant voltage and gate-source voltage V_{GS} applied as a sweep. V_{DS} is set at −0.6 V. V_{GS} varies from −0 to −0.6 V as a pulsed signal with a pulse width of 0.202 s. The pulsed measurement procedure has been proven to minimize the bias stress effect on the device [9]. Both drain-source I_{DS} and gate I_{GS} currents are measured (Fig. 7) .

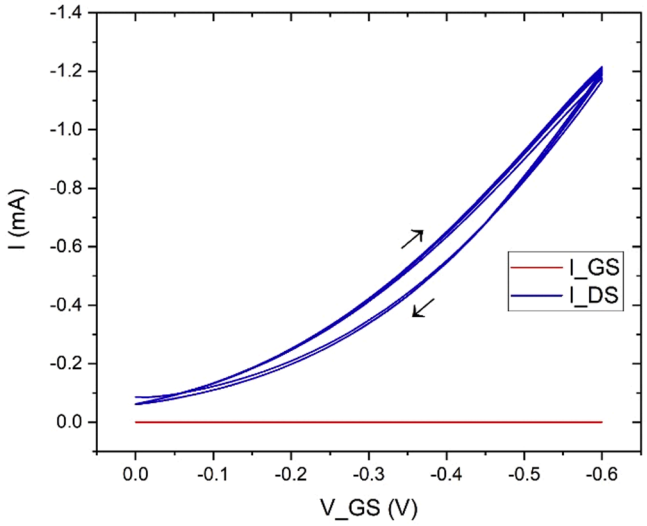

Fig. 7. Typical transcharacteristics curve of the device. V_{DS} is set to −0.6 V . Gate current I_{GS} (in red) is four orders of magnitude lower than drain-source current I_{DS} (in blue). The arrows show forward, and backward voltage sweep which creates hysteresis.

3.2. Preliminary stability check

In our prior work, the main concern regarding the device described in [23] are instability and inconsistency in current values during the replicated measurements for different devices and gates due to aggregation bumps created while drying the chip very fast. Another problem was due to the active gates area being defined by the open windows in the PDMS microfluidics instead of being uniquely patterned on the electrodes. Indeed, without patterned gate electrodes, the sensing area of the electrode may be modified by uncontrolled movements of the PDMS wall during liquids injection which then changes the current values. This affects the biomarkers detection sensitivity. An important milestone has been achieved by solving these problems with the aforementioned solutions that are i) changing the deposition technique (from spin coating to ink-jet) of the semiconductor to gain a high stability and repeatability and ii) patterning the gate electrode to reach high selectivity and comparable devices from batch to batch.

Preliminary tests were conducted to ensure device stability before bio-detection, focusing on storage conditions since fabrication and testing took place in separate labs. Devices were tested in both vacuum and PBS buffer, with those stored in PBS showing greater stability, as demonstrated in Figure S4a. Stability was assessed by measuring the variation in maximum current between repeated tests without analyte injection, with closer values to zero indicating better stability. Devices were considered stable if their signal variation was under 5 %, and Bovine Serum Albumin (BSA) was tested at different concentrations as a preliminary biosensing measurements (Figure S5).

3.3. Biomarker detection (Ang2)

The device was employed for Ang2 detection. As described before, surface of Au-gate has been functionalized by Anti-Ang2 antibody to allow for better bonding between the gate and target due to the high specificity antigen-antibody of the binding. Different Ang2 concentrations were measured: 1 pM, 10 pM, 25 pM, 40 pM, 50 pM, 75 pM, 100 pM and 150 pM. On average, four new devices were tested for every concentration. PBS 0.01x was used during stabilization and washing procedures. The current signal can be also described as a Hill-Langmuir isotherm behavior [25]. The data is plotted by the Hill-Langmuir model:

$$\frac{\Delta I}{I} = Smax\frac{c^n}{(K_d + c^n)} \tag{2}$$

where c is the Ang2 solution concentration, $\frac{\Delta I}{I}$ is the current sensitivity signal in stationary conditions, Smax, n and Kd are the parameters of the

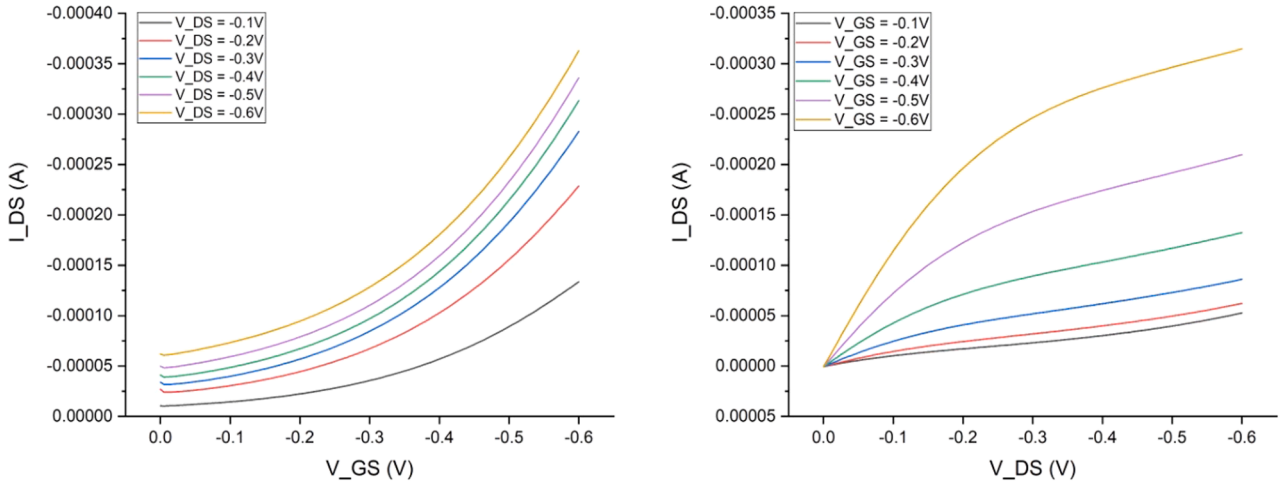

Fig. 6. Electrical characterization of the devices. (a) transcharacteristics and (b) output characteristics.

Hill-Langmuir model. From the model (Fig. 8) it is possible to retrieve the maximum sensitivity value $\frac{\Delta I}{I\_MAX} = Smax$ that is of 0.18645 for 250pM. Kd represents the ratio between constants of backward desorption reaction and forward adsorption reaction coefficients between Ang2 and anti-antibody on the gate. The Kd value obtained from the plot is 7.51×10^{-11} similar to the value in the picomolar range (8.6×10^{-11}) reported in [26]. Most antibodies have Kd values in the low micromolar (10^{-6}) to nanomolar (10^{-7} to 10^{-9}) range, high affinity antibodies are generally considered to be in the low nanomolar range (10^{-9}) [27], and very high-affinity antibodies being in the picomolar (10^{-12}) range. The Hill coefficient n that describes the slope of the binding curve in a log-log plot and reflects the nature of binding interactions has a value 1.16871, meaning that there is a positive cooperativity between binding cites.

All bar graph data are presented as the mean ± standard deviation for all experiments per concentration or gate. Significance was measured as indicated for each experiment, with two-way or one-way ANOVA followed by pairwise comparison with Tukey's multiple comparisons test using OriginPro (Fig. 9): $*p < 0.05$, $**p < 0.01$, $***p < 0.001$.

In addition, negative control experiments for selectivity were also performed. Measurements of samples containing a different tumor biomarker, vascular endothelial growth factor (VEGF), in order to check selectivity of the biosensor. VEGF is a crucial factor for the induction of the angiogenic program to sustain the growth and metastasis of solid tumors [28]. In this case, the device showed high selectivity even for the concentration of VEGF as high as 100pM. Since the signal of the sensing gate kept value close to zero after the incubation, thus confirming the selectivity of the device (Fig. 10).

The concentration of Ang2 in human plasma measured with ELISA has been reported in numerous studies, resulting in approximately 1–3 ng/mL (18–54 pM) in healthy controls and higher concentrations in disease subjects [29]. To accurately measure these concentrations, the platform underwent optimization. The purpose of the optimization was to enhance the device's overall performance, reliability, sensitivity, ensuring consistent and accurate detection of Ang2 within the range of interest. The ability of the instrument to detect Ang2 concentrations as low as 10 pM in the diluted phosphate buffer has demonstrated its sensitivity. This is a significant result since it proves the platform's ability to properly recognize the relevant range of Ang2 concentrations

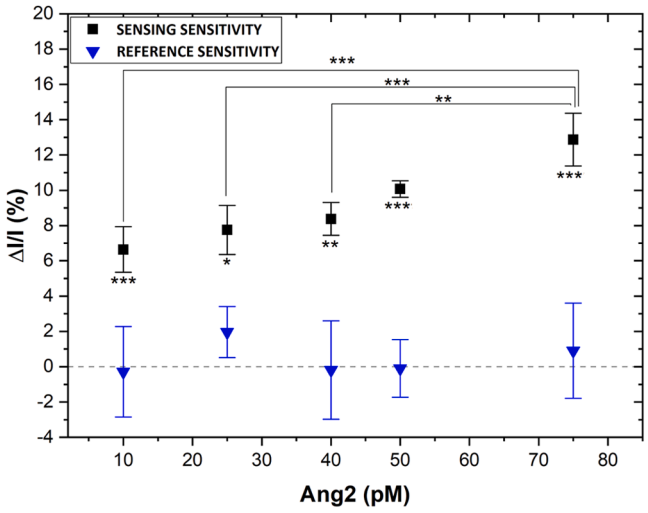

Fig. 9. Comparison of the signal ΔI/I in the range of interest at 10, 25, 40, 50, 75 pM concentration of Ang2 in human plasma is approximately 1–3 ng/mL (18–54 pM) in healthy controls [30] . Tukey's multiple comparisons test $*p < 0.05$, $**p < 0.01$, $***p < 0.001$. Although, the sensor does not show significant difference between 75 and 50pM, there is a significant difference in current between 75pM and 10, 25 and 40pM. Also, the device shows a significant divergence between reference and sensing gate for each concentration, presented by asterisks under each sensing sensitivity bar.

at least considering samples with a low level of matrix complexity (i.e., diluted PBS). The next step would be to use this platform to examine actual patient liquid biopsy samples and/or combine the developed platform with a biological 3D advanced model of a specific disease of interest to evaluate relevant biomarkers. Liquid biopsy has a huge potential and application for diagnosis, monitoring, and therapy of the reference diseases [30]. By modifying the functionalization of its gate electrodes, the device may be designed to detect a wide range of analytes (substances or molecules of interest). These changes would allow it to identify biomarkers or molecules at relevant concentrations linked to various diseases or medical disorders in samples of real life as well as in samples obtained from in vitro biological models of disease for precision

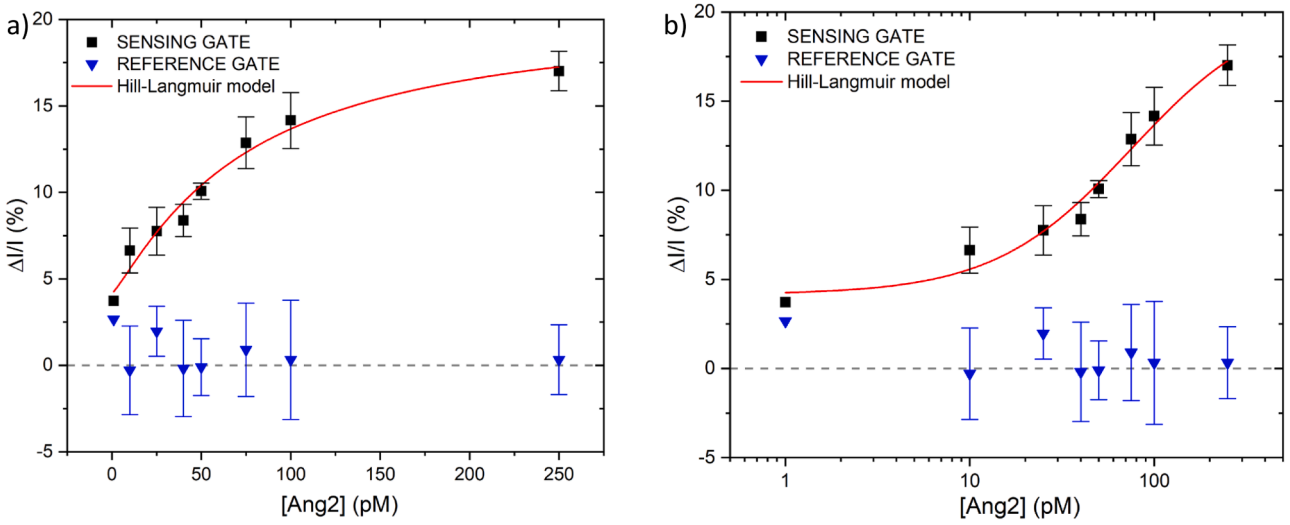

Fig. 8. a) linear plot and b) logarithmic of the obtained signal ΔI/I is reported in the figure above. Error bars are calculated as the mean value of the signal ΔI/I for between devices. The results show that the signal increases with the Ang2 concentration, with a maximum variation registered at around 14 % with respect to the starting level for a concentration of 100 pM of analyte. Signal of the reference gate is close to zero, thus confirming that the biosensor was not contaminated during the Ang2 exposure. The sensitivity of the EGOT is maximized in the range between 25 pM and 75 pM of concentrations, in which the greatest variation of the output signal is recorded. The signal from the sensing gate is fitted with Hill-Langmuir model: Absorption isotherms of Ang2 immobilization curve by fitting obtained data from different Ang2 concentrations measurements.

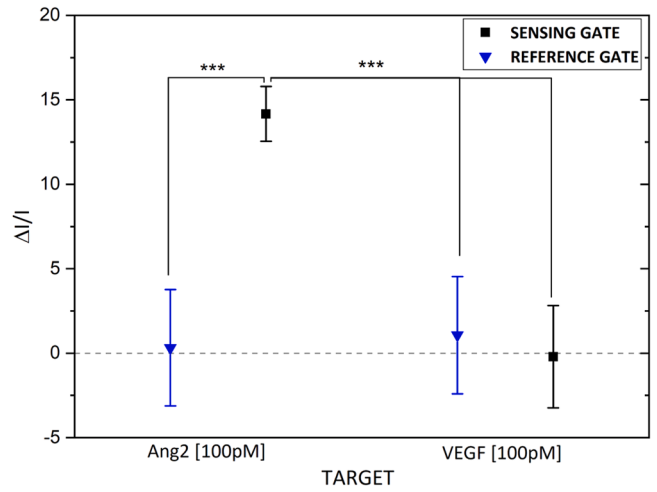

Fig. 10. After the flux of sensing gate with VEGF, the signal remained close to zero – no target detection. On the other hand, signal of the sensing gate increased after exposure with Ang2, thus confirming selectivity. Tukey's multiple comparisons test $^{*}p < 0.05$, $^{**}p < 0.01$, $^{***}p < 0.001$ shows a significant difference in current measured by the sensing gates after angiopoietin2 and VEGF treatment.

medicine purpose.

4. Conclusion

This work was focused on optimizing a microfluidic platform with an integrated EGOT device to detect a specific biomarker. In our previous works we investigated EGOTs stability towards electrical bias stress and introduced the refence electrode and the contamination free platform. In this paper, a significant impact on device stability and sensitivity were reached by introducing four important novelties, which are i) P3CPT inkjet deposition method, ii) patterned gate electrodes, iii) 3D printed top cover with fixed contacts and iv) new measurement protocol with a stabilization time before measurements. These optimizations contribute to more robust and reliable biosensing. Performed measurements have proven the platform's ability to detect Ang2 tumor biomarker at concentrations as low as 10 pM in a dilute phosphate buffer. Also, the platform's ability to detect a broader range of biomolecules increases its versatility for multi-analyte detection.

Our technology offers enormous potential in biomedical applications for early detection and monitoring of tumor biomarkers that can highly impact on patient outcomes and treatment options. Indeed, this platform may be modified to work as a flexible diagnostic tool in a variety of medical environments by modifying the gate electrode functionalization to target analytes associated with distinct disorders.

Nevertheless, the improvement of the Ang2 detecting device is crucial for enhancing its potential medical diagnostic applications such as continuing to enhance the device's specificity to accurately identify Ang2 in the presence of different molecules in complex biological samples. Also, long-term stability of the device is still a great concern. The device must be stable over a long time. This is essential for maintaining precision and reliability over time, especially if the device is being used to monitor an ongoing medical condition. Another point that can be improved is the device's detection and response time. The technology may be more useful for clinical application if the time it takes to provide outcomes is reduced. The effective functioning of the device in emergency and point-of-care settings may increase with faster detection.

Funding sources

This project is supported by the European Union – NextGenerationEU for funding the project "RAISE - Robotics and AI for Socio-economic Empowerment".

This work was supported by the National Plan for Complementary Investments to the NRRP, project "D34H—Digital Driven Diagnostics, prognostics and therapeutics for sustainable Health care" (project code: PNC0000001), Spoke 4 funded by the Italian Ministry of University and Research.

CRediT authorship contribution statement

Jovana Babic: Writing – original draft, Methodology, Investigation, Data curation. **Alberto Ballesio:** Supervision, Methodology. **Francesca Frascella:** Writing – review & editing, Validation, Supervision, Conceptualization. **Lucia Napione:** Validation, Formal analysis. **Mattia Pagani:** Methodology, Investigation. **Matteo Parmeggiani:** Validation, Methodology, Investigation. **Simone Luigi Marasso:** Writing – review & editing, Supervision, Methodology, Conceptualization.

Declaration of competing interest

The authors declare that they have no known competing financial interests or personal relationships that could have appeared to influence the work reported in this paper.

Supplementary materials

Supplementary material associated with this article can be found, in the online version, at doi:10.1016/j.snr.2025.100341.

Data availability

Data will be made available on request.

References

[1] H. Sung, et al., Global Cancer statistics 2020: GLOBOCAN estimates of incidence and mortality worldwide for 36 cancers in 185 countries, CA Cancer J. Clin. 71 (3) (2021) 209–249, https://doi.org/10.3322/caac.21660. May.
[2] J.W.A. Findlay, et al., Validation of immunoassays for bioanalysis: a pharmaceutical industry perspective, J. Pharm. Biomed. Anal. 21 (6) (2000) 1249–1273, https://doi.org/10.1016/S0731-7085(99)00244-7. Jan.
[3] B.V. Chikkaveeraiah, A.A. Bhirde, N.Y. Morgan, H.S. Eden, X. Chen, Electrochemical immunosensors for detection of cancer protein biomarkers, ACS. Nano 6 (8) (2012) 6546–6561, https://doi.org/10.1021/nn3023969. Aug.
[4] A. Pappa, et al., Organic transistor arrays integrated with finger-powered microfluidics for multianalyte saliva testing, Adv. Healthc. Mater. 5 (17) (2016) 2295–2302, https://doi.org/10.1002/adhm.201600494. Sep.
[5] V.F. Curto, et al., Organic transistor platform with integrated microfluidics for in-line multi-parametric in vitro cell monitoring, Microsyst. Nanoeng. 3 (1) (Aug. 2017) 17028, https://doi.org/10.1038/micronano.2017.28.
[6] A. Koklu, et al., Microfluidics integrated n-type organic electrochemical transistor for metabolite sensing, Sens. Actuators. B Chem. 329 (2021) 129251, https://doi.org/10.1016/j.snb.2020.129251. Feb.
[7] J. Borges-González, C.J. Kousseff, C.B. Nielsen, Organic semiconductors for biological sensing, J. Mater. Chem. C. Mater. 7 (5) (2019) 1111–1130, https://doi.org/10.1039/C8TC05900D.
[8] H. Toss, et al., On the mode of operation in electrolyte-gated thin film transistors based on different substituted polythiophenes, Org. Electron. 15 (10) (2014) 2420–2427, https://doi.org/10.1016/j.orgel.2014.06.017. Oct.
[9] M. Segantini, et al., Investigation and modeling of the electrical bias stress in electrolyte-gated organic transistors, Adv. Electron. Mater. 8 (7) (2022), https://doi.org/10.1002/aelm.202101332. Jul.
[10] P. D'Angelo, et al., Homocysteine solution-induced response in Aerosol jet printed OECTs by means of gold and platinum gate electrodes, Int. J. Mol. Sci. 22 (21) (2021) 11507, https://doi.org/10.3390/ijms222111507. Oct.
[11] V. Preziosi, et al., Organic electrochemical transistors as novel biosensing platforms to study the electrical response of whole blood and plasma, J. Mater. Chem. B 10 (1) (2022) 87–95, https://doi.org/10.1039/D1TB01584B.
[12] M. Barra, et al., Organic electrochemical transistor immuno-sensors for spike protein early detection, Biosensors. (Basel) 13 (7) (2023) 739, https://doi.org/10.3390/bios13070739. Jul.
[13] V. Preziosi, et al., Immuno-sensing at ultra-low concentration of TG2 protein by organic electrochemical transistors, Biosensors. (Basel) 13 (4) (2023) 448, https://doi.org/10.3390/bios13040448. Mar.
[14] D. Gentili, et al., Integration of organic electrochemical transistors and immuno-affinity membranes for label-free detection of interleukin-6 in the physiological

concentration range through antibody–antigen recognition, J. Mater. Chem. B 6 (33) (2018) 5400–5406, https://doi.org/10.1039/C8TB01697F.
[15] M.Y. Lee, H.R. Lee, C.H. Park, S.G. Han, J.H. Oh, Organic transistor-based chemical sensors for wearable bioelectronics, Acc. Chem. Res. 51 (11) (2018) 2829–2838, https://doi.org/10.1021/acs.accounts.8b00465. Nov.
[16] M.L. Hammock, O. Knopfmacher, B.D. Naab, J.B.-H. Tok, Z. Bao, Investigation of protein detection parameters using nanofunctionalized organic field-effect transistors, ACS. Nano 7 (5) (2013) 3970–3980, https://doi.org/10.1021/nn305903q. May.
[17] M. Sensi, et al., Anti-drug antibody detection with label-free electrolyte-gated organic field-effect transistors, Chem. Commun. 57 (3) (2021) 367–370, https://doi.org/10.1039/D0CC03399E.
[18] P. D'Angelo et al., "Nanomolar detection of the antitumor drug tamoxifen by flexible organic electrochemical devices," 2018, p. 020015. doi: 10.1063/1.5047769.
[19] M. Segantini, et al., Design of a contamination-free microfluidic device for Electrolyte-gated organic Field-effect transistor (EGOFET) biosensors, Biomed. Sci. Eng. 2 (1) (2021), https://doi.org/10.4081/bse.191. Sep.
[20] R.G. Akwii, M.S. Sajib, F.T. Zahra, C.M. Mikelis, Role of angiopoietin-2 in vascular physiology and pathophysiology, Cells 8 (5) (2019) 471, https://doi.org/10.3390/cells8050471. May.
[21] X. Yu, F. Ye, Role of angiopoietins in development of cancer and neoplasia associated with viral infection, Cells 9 (2) (2020) 457, https://doi.org/10.3390/cells9020457. Feb.
[22] C. Antoniotti, et al., Early modulation of angiopoietin-2 plasma levels predicts benefit from regorafenib in patients with metastatic colorectal cancer, Eur. J. Cancer 165 (2022) 116–124, https://doi.org/10.1016/j.ejca.2022.01.025. Apr.
[23] M. Segantini, et al., Design of a portable microfluidic platform for EGOT-based in liquid biosensing, Sensors 22 (3) (2022) 969, https://doi.org/10.3390/s22030969. Jan.
[24] V. Frantellizzi, et al., 99mTc-labeled keratin gold-nanoparticles in a nephron-like microfluidic chip for photo-thermal therapy applications, Mater. Today Adv. 16 (2022) 100286, https://doi.org/10.1016/j.mtadv.2022.100286. Dec.
[25] M. Jozwik, K. Kaczmarski, R. Freitag, Evaluation of the Langmuir formalism for modeling the adsorption isotherms of proteins and polyelectrolytes in simulations of ion exchange chromatography, Chem. Eng. Technol. 28 (11) (2005) 1346–1359, https://doi.org/10.1002/ceat.200500112. Nov.
[26] J.L. Brown, et al., A Human monoclonal anti-ANG2 antibody leads to broad antitumor activity in combination with VEGF inhibitors and chemotherapy agents in preclinical models, Mol. Cancer Ther. 9 (1) (2010) 145–156, https://doi.org/10.1158/1535-7163.MCT-09-0554. Jan.
[27] S.-H. Park, et al., Isolation and characterization of a monobody with a fibronectin domain III scaffold that specifically binds EphA2, PLoS. One 10 (7) (2015) e0132976, https://doi.org/10.1371/journal.pone.0132976. Jul.
[28] L. Napione, et al., Unraveling the influence of endothelial cell density on VEGF-A signaling, Blood 119 (23) (2012) 5599–5607, https://doi.org/10.1182/blood-2011-11-390666. Jun.
[29] G. Thurston, C. Daly, The complex role of angiopoietin-2 in the angiopoietin-tie signaling pathway, Cold. Spring. Harb. Perspect. Med. 2 (9) (2012) a006650, https://doi.org/10.1101/cshperspect.a006650 a006650Sep.
[30] X. Li, et al., Liquid biopsy of circulating tumor DNA and biosensor applications, Biosens. Bioelectron. 126 (2019) 596–607, https://doi.org/10.1016/j.bios.2018.11.037. Feb.